

# Dissolvable Probiotic-Powered Biobatteries: A Safe and Biocompatible Energy Solution for Transient Applications

Maryam Rezaie, Maedeh Mohammadifar, and Seokheun Choi\*

For decades, science fiction has imagined electronic devices that spring to life on demand, function as programmed, and then vanish without a trace. Today, transient and bioresorbable electronics are making that vision a reality, sparking revolutionary progress in biomedicine, environmental stewardship, and hardware security. Yet one critical barrier remains: a fully transient power source with the same disappearing act. Microbial-based biobatteries have emerged as strong contenders, harnessing the power of microorganisms—found virtually everywhere—as natural biocatalysts. However, toxicity and health risks have limited these systems to single-use, often incinerable applications. Here, a transformative approach: a transient biobattery powered by commercially available probiotics that dissolves harmlessly is introduced, releasing only beneficial microbes. Fabricated on water-soluble or pH-responsive substrates, this biobattery capitalizes on a 15-strain probiotic blend to generate electricity across diverse electrode materials. By manipulating device length or encapsulating it with pH-sensitive polymers, power delivery can be fine-tuned from 4 min up to over 100 min. A single module outputs 4  $\mu\text{W}$  of power, 47  $\mu\text{A}$  of current, and an open-circuit voltage of 0.65 V. This groundbreaking design ushers in a new era of safe, effective transient bioenergy systems, opening unprecedented opportunities in biomedical implants, environmental sensors, and disposable electronics.

self-destructs in 5 s to protect sensitive information. This concept has been recognized in engineering and science as a distinct class of advanced technologies known as “Transient Electronics.”<sup>[1,2]</sup> By definition, transient electronics are designed for short-term, mission-specific operation, after which they self-destruct and cease to function.<sup>[1]</sup> In biomedical and environmental applications, an additional requirement is that these devices dissolve and be resorbed in situ, leaving minimal, harmless residues—thus eliminating the need for retrieval.<sup>[3,4]</sup> Consequently, the term “Bioresorbable Electronics” has emerged to describe transient devices specifically engineered for biomedical and environmental applications, offering dissolvability, along with biocompatibility, biosafety, and environmental friendliness.<sup>[5,6]</sup>

The remarkable ability of these devices to disappear without leaving an environmental footprint has paved the way for a new field known as “Green Electronics” or “Sustainable Electronics.”<sup>[7–9]</sup> This advancement offers a promising solution to

## 1. Introduction

In the *Mission Impossible* film series, a device delivering mission instructions to Ethan Hunt, played by Tom Cruise,

the critical global challenge of electronic waste (e-waste), which is exacerbated by rapid technological upgrades and obsolescence. However, while green electronics may take months for environmental microorganisms to break down, transient and bioresorbable electronics must adhere to far more rigorous standards—disintegrating within hours or even minutes once their short-term missions are accomplished. In this context, it is important to clarify a common misconception found in various research and review articles: the primary objective of transient and bioresorbable electronics is not merely the reduction of e-waste. Rather, their fundamental purpose is to enable short-term, predefined operation, after which they disintegrate when no longer needed. Their transient nature is designed to serve applications where retrieval is impractical or undesirable, such as temporary medical implants, environmental sensors, or disposable security devices.<sup>[1,3,6]</sup>

In developing fully transient electronic systems, a critical challenge lies in integrating a suitable transient power source.<sup>[10,11]</sup> Such a power source is essential for enabling an entirely transient system capable of independent and self-sustaining operation. Conventional power solutions—such as lithium-ion batteries, supercapacitors, and other common battery technologies—have increasingly come under scrutiny due to their reliance on

M. Rezaie, M. Mohammadifar, S. Choi  
Bioelectronics & Microsystems Laboratory  
Department of Electrical & Computer Engineering  
State University of New York at Binghamton  
Binghamton, NY 13902, USA  
E-mail: [sechoi@binghamton.edu](mailto:sechoi@binghamton.edu)

S. Choi  
Center for Research in Advanced Sensing Technologies & Environmental Sustainability  
State University of New York at Binghamton  
Binghamton, NY 13902, USA

 The ORCID identification number(s) for the author(s) of this article can be found under <https://doi.org/10.1002/smll.202502633>

© 2025 The Author(s). Small published by Wiley-VCH GmbH. This is an open access article under the terms of the [Creative Commons Attribution-NonCommercial-NoDerivs](#) License, which permits use and distribution in any medium, provided the original work is properly cited, the use is non-commercial and no modifications or adaptations are made.

DOI: 10.1002/smll.202502633

nonbiodegradable and potentially toxic inorganic materials, energy-intensive manufacturing, and hazardous waste generation.<sup>[12]</sup> Although some research efforts have explored transient power sources and energy storage devices,<sup>[10,11,13,14]</sup> these technologies remain in their early stages and are often unsuitable for bioresorbable applications because of toxic components or reactive properties. In contrast to standard electronics requiring high power and long operational lifetimes, transient systems typically function for shorter periods at lower power levels. In this setting, low-power energy harvesting techniques have emerged as a promising alternative for transient and bioresorbable electronics.<sup>[15,16]</sup> By reducing dependence on hazardous materials and enabling simplified, eco-friendly manufacturing processes, these techniques address key environmental and safety concerns. Furthermore, energy harvesters provide a maintenance-free, sustainable power supply, making them particularly advantageous for harsh or unattended environments where fully transient electronics are most needed.

Among various energy harvesting methods—such as solar, thermoelectric, mechanical, hygroscopic, and radiofrequency-based systems—microbial fuel cells (MFCs), also known as microbe-powered biobatteries, stand out as especially sustainable power sources for transient electronics.<sup>[17,18]</sup> Microbe-powered biobatteries convert environmental resources into electrical energy through the metabolic activities of microbes, which serve as environmentally friendly catalytic materials.<sup>[19,20]</sup> These microorganisms are ubiquitous and can maintain their viability through abundant, renewable surrounding resources.<sup>[17]</sup> Beyond environmental microbes, even human skin and gut microorganisms have successfully been employed as energy-producing biocatalysts for powering wearable and ingestible applications.<sup>[21–24]</sup> Furthermore, microbes in natural settings can adapt to harsh or fluctuating conditions by developing robust survival strategies, making microbe-powered biobatteries particularly effective in diverse environments.<sup>[17,18]</sup> Their self-growing, self-assembling, self-repairing, and self-maintaining characteristics further enhance continuous and reliable power generation, positioning microbe-powered biobatteries as an ideal choice for powering transient electronic devices in real-world scenarios.

Many microbe-powered biobatteries have been successfully demonstrated as stand-alone power sources for transient and other eco-friendly electronic applications.<sup>[25–30]</sup> However, concerns about microbial cytotoxicity and associated health risks have largely restricted these devices to disposable applications, typically requiring incineration for safe disposal.<sup>[31]</sup> This constraint has prevented the development of dissolvable or resorbable biobatteries, which would be more practical for healthcare and environmental applications. Although the microorganisms employed in these biobatteries are often Generally Recognized as Safe (GRAS), they can still present potential risks—for instance, if they are unintentionally released into the environment, proliferate in unforeseen ecological niches, or interact with immunocompromised individuals. Consequently, their use in biomedical and environmental transient systems, where preloaded microbes would be released following a programmed operational period, remains impractical under current safety and regulatory standards.

Here, we present a groundbreaking dissolvable biobattery that prioritizes biosafety and biocompatibility by leveraging commer-

cially available probiotics as on-demand biocatalysts. Harnessing the well-established safety and health benefits of these probiotic strains, the biobattery is ideally suited for transient and bioresorbable applications in both medical and environmentally sensitive settings. Constructed with biodegradable components on a water-soluble paper substrate, the biobattery disintegrates harmlessly upon exposure to water (Figure 1a). As it dissolves, encapsulated probiotics are released from their protective layers, metabolizing available substrates to produce significant electrical output—marking the first demonstration of electrogenic capabilities in probiotics for power generation. To enable scalable and low-cost production, the device can be printed or pencil-drawn on dissolvable paper with varying lengths or numbers of serpentine electrodes within capillary microfluidic channels (Figure 1b). Its operational lifetime is finely regulated by a bottom-up dissolution process, allowing synchronized power generation over a predefined interval. To further refine activation precision and transient control, the biobattery is enveloped in a pH-sensitive membrane, ensuring reliable and sustained performance (Figure 1c). Specifically, a low pH-sensitive membrane enables activation exclusively in acidic environments, such as the stomach or environmentally polluted areas with acid contamination. Moreover, the low pH-sensitive membrane prevents premature dissolution during fabrication. By encapsulating the water-soluble paper substrate, the pH-sensitive membrane ensures structural integrity even when liquid conductive materials—such as polypyrrole (PPy) conjugated with ZnO<sub>2</sub> nanoparticles—are applied, preserving electrode integrity for optimal power performance. Once deployed in a low-pH setting, the membrane selectively dissolves, activating the probiotics and electrodes in a timely, controlled manner, and ultimately leading to the complete dissolution of the biobattery upon the dissolution of its paper substrate. This targeted exposure maximizes electrical output within the intended operational window, prevents unwanted leakage or early depletion of active materials, and ensures consistent, high-performance power generation.

Overall, this dissolvable biobattery capitalizes on the inherent safety and biocompatibility, of probiotics to deliver a practical, eco-friendly, and easily fabricated transient power source. By expanding the potential of transient electronic technologies, this innovation advances next-generation medical, environmental, and bioresorbable applications—offering a versatile, controlled, and sustainable solution for power generation.

## 2. Results and Discussion

### 2.1. Microbe-Powered Biobatteries on Dissolvable Paper with Tunable Dissolution

Microbe-powered biobatteries rely on four primary components for operation: an anode coated with biocatalysts, a reservoir for microbial feed, an ion-exchange membrane, and a cathode containing catalysts.<sup>[32]</sup> When a suitable organic food source is metabolized by the microbial biocatalysts, redox reactions generate electrons and protons. The electrons travel through an external circuit to power a load, while the protons migrate through the ion-exchange membrane to the cathode, where they recombine with electrons in a catalytic reaction, thus completing the circuit.

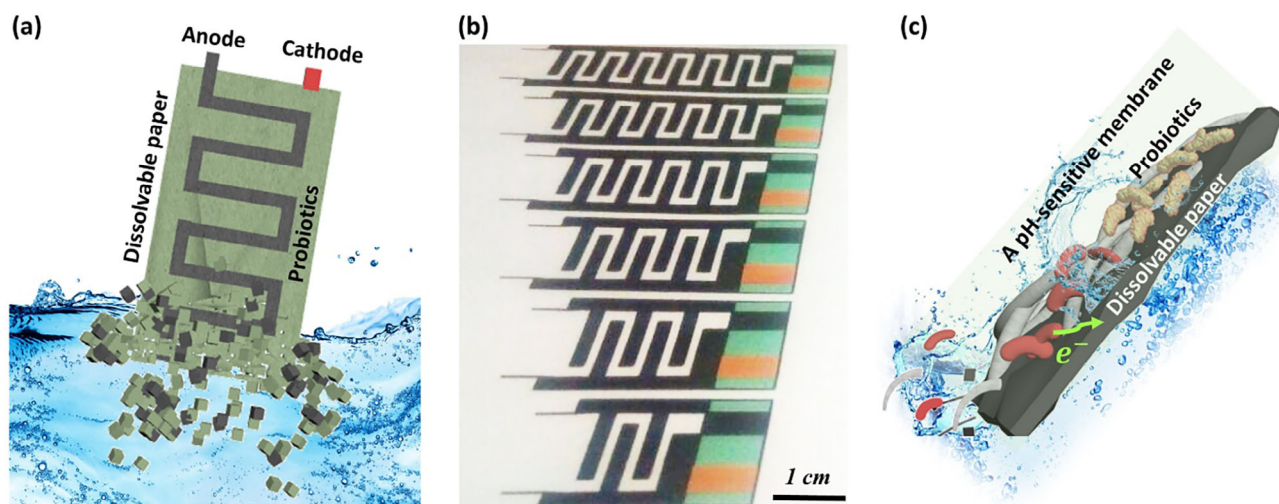


**Figure 1.** A transient probiotic-powered biobattery on a dissolvable paper substrate. a) Schematic representation of the transient biobattery, designed on a dissolvable paper platform and powered by probiotics. b) Demonstration of the biobattery's printability and scalability, showcasing variations in electrode length and the number of serpentine electrodes integrated within capillary microfluidic channels. c) An optimized version of the transient biobattery, encapsulated in a low-pH-sensitive polymer for enhanced control over dissolution and activation.

Papers have been widely adopted for these systems owing to their low cost, flexibility, lightweight nature, and high surface area.<sup>[27,29]</sup> Moreover, their intrinsic capillary action and compatibility with liquid-phase functional materials render them particularly advantageous for microbe-powered devices. Post-use disposal is straightforward via incineration, eliminating the risk of bacterial contamination.<sup>[31]</sup> With the increasing focus on paper-based electronics—or papertronics—those biobatteries are gaining recognition as viable power sources for disposable, environmentally-friendly electronic systems.<sup>[25,33,34]</sup> However, conventional cellulose papers, although biocompatible, degrade relatively slowly<sup>[28]</sup>—over several months—making them unsuitable for transient and bioresorbable applications.

To address this limitation, we investigate the feasibility of fabricating dissolvable biobatteries using commercially available water-soluble paper (SmartSolve Industries), enabling on-demand transient power through tunable dissolution rates (Figure 2a). By tailoring the solubility characteristics of the substrate, we aim to create biobattery platforms that integrate seamlessly with transient electronic systems while ensuring safe disposal. As a proof-of-concept, we employed *Shewanella oneidensis* MR-1, a well-characterized exoelectrogen, to validate a prototype transient microbial biobattery.<sup>[35]</sup> Although *S. oneidensis* is extensively used in biobatteries, our ultimate goal is to transition to biosafe probiotics for enhanced safety and biocompatibility in real-world applications. Here, transient biobatteries were constructed on a single-sheet, water-soluble paper substrate with four vertically arranged functional layers: the anode, the microfluidic reservoir, the ion-exchange membrane, and the cathode (Figure 2a). The serpentine microfluidic reservoir, extending through the entire thickness of the paper, was delineated by hydrophobic wax boundaries to enable controlled substrate degradation and simultaneous power generation upon water exposure. On one side, a pencil-drawn graphite layer served as the anode, while on the opposite side, a wax-based ion-exchange

membrane was strategically printed before adding a Prussian blue cathode (Figure 2b). Our previous studies have extensively characterized this wax-based membrane, confirming its efficiency in facilitating ion transport and enhancing electrochemical performance.<sup>[29]</sup> The liquid-free nature of the pencil-drawn anode prevented paper dissolution during fabrication, and the wax layer protected the substrate from dissolving when the liquid cathodic solution was applied. *S. oneidensis* cells were first freeze-dried and then pre-inoculated into the patterned reservoir, enabling their reactivation once water penetrates the reservoir. The freeze-drying technique preserved microbial viability for long-term storage, preventing degradation or denaturation.<sup>[36,37]</sup> During operation, only the bottom portion of the device was submerged in water (Figure 2a). As water traveled upward through the serpentine microfluidic reservoir channel via capillary action, the device gradually disintegrated while simultaneously generating power. Real-time voltage and current measurements were continuously recorded to evaluate power output and confirm the functionality of this transient, paper-based microbial biobattery.

In this study, six microfluidic channel designs were evaluated, each with a different number of serpentine curves ( $n = 1$ –6). The open-circuit voltage (OCV) was monitored continuously during the dissolution process. As shown in Figure 2c, increasing the channel length prolonged the device's operational time. For instance, the device with a single serpentine curve ( $n = 1$ ) operated for only 4 min, whereas the device with six curves ( $n = 6$ ) produced a voltage for over 22 min. To further investigate the current output, the  $n = 6$  device was tested with three different resistors (100, 10, and 1 k $\Omega$ ) (Figure S1a, Supporting Information). The device successfully operated for 25 min and generated current outputs corresponding to each resistor value (Figure S1a, Supporting Information). Figure S1b (Supporting Information) presents the polarization curves and power outputs of devices with  $n = 4$  and  $n = 6$ . The  $n = 6$  device achieved a maximum power of 0.5  $\mu$ W with a current of 13  $\mu$ A. It is important to note that the low performance, attributed to high internal resistance, primarily arises



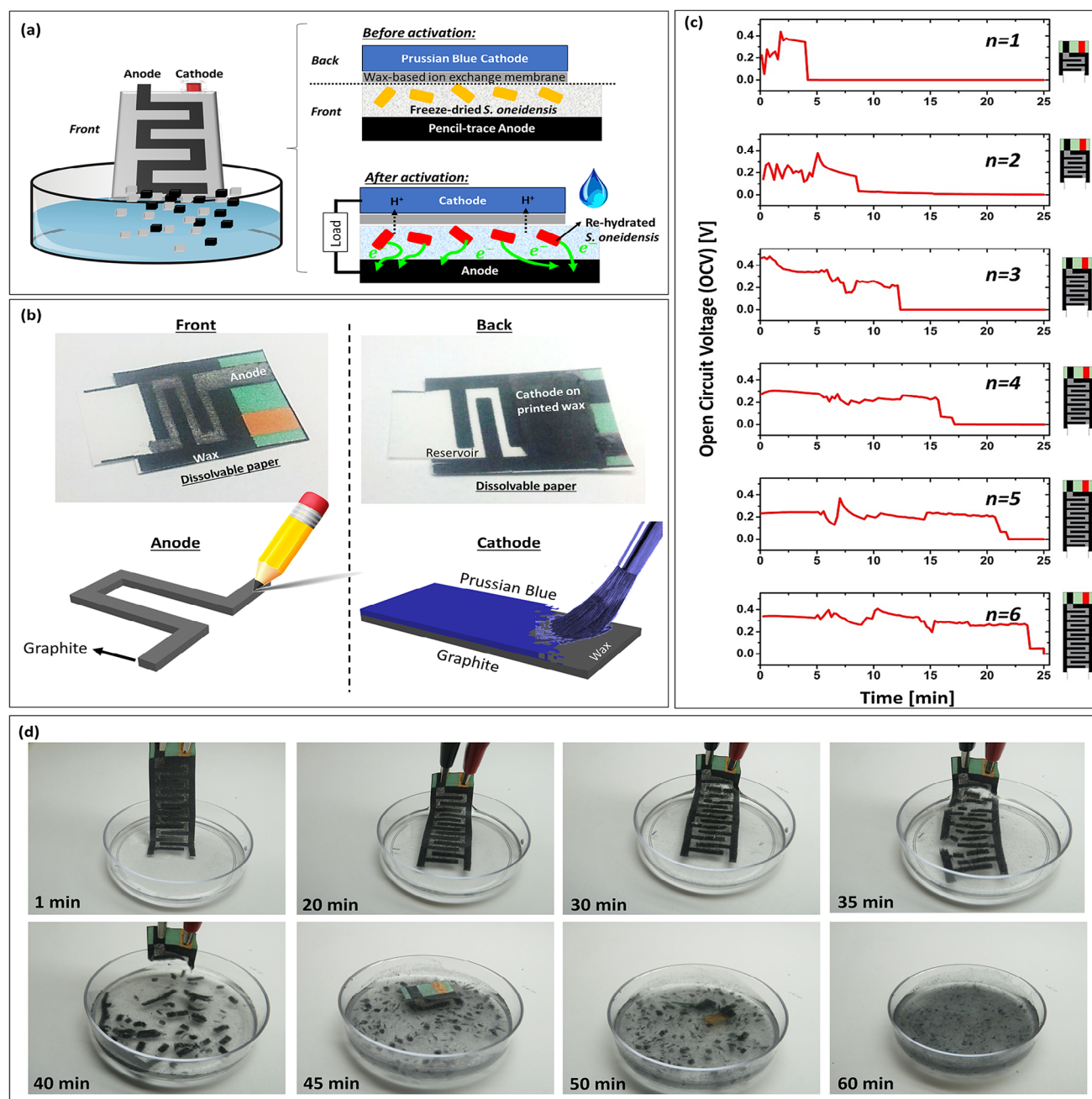


**Figure 2.** A microbe-powered biobattery on dissolvable paper with tunable dissolution. a) Schematic illustrations of the biobattery and its operating mechanism. b) Front and back views of the bio battery, along with key fabrication details. c) Performance evaluation showing the operational duration of devices with varying numbers of serpentine curves ( $n = 1-6$ ). d) Transience test of the device ( $n = 6$ ) in water, demonstrating complete dissolution within 60 min.

from the non-conductive anodic reservoir and the use of pencil graphite as the electrode material. The majority of electrogenic bacteria remain within the non-conductive reservoir, while only a small fraction near the graphite electrode can effectively transfer electrons.

All components of the biobattery—including the substrate, printed wax boundaries and membranes, pencil-drawn electrodes, and Prussian Blue cathode—were designed to disinte-

grate in water as the substrate dissolved. The water-soluble paper is primarily derived from bio-based materials, such as wood pulp fibers combined with a natural cellulose component. Upon contact with water, the cellulose dissolves, causing the wood pulp fibers to disperse into microfibrils. This process is facilitated by the hydrophilic nature of cellulose, which promotes interaction with water molecules and leads to the breakdown of the paper structure. As the fibers disperse, an environmentally friendly

disposal route is achieved. Pencil graphite and Prussian Blue are biocompatible; however, the wax used in this study is not strictly biocompatible. Despite this, its minimal use reduces potential environmental impact, and other biocompatible waxes—such as those derived from palm oil or BIOMERE—could serve as suitable replacements. In this work, the primary focus was on the dissolvability of the biobattery for transient applications. The paper-based substrate completely dissolved within 2 min, whereas the wax-printed boundaries and pencil-drawn traces required additional time to disintegrate. Figure 2d depicts the dissolution process of the  $n = 6$  biobattery in water at room temperature, with complete disintegration occurring within  $\approx 60$  min. Throughout the dissolution process, SEM imaging at various time points captured the progressive breakdown of the biobattery structure (Figure S2, Supporting Information).

This study introduces a simple, cost-effective, and environmentally sustainable approach to transient microbial biobatteries. By initially validating the concept with *S. oneidensis* and paving the way for biosafe probiotic alternatives, this research establishes a critical step toward water-dissolvable and on-demand energy solutions for transient electronic applications.

## 2.2. Evaluating Probiotic Electrogenicity and Boosting It with Novel Electrodes

Previous research on single-use, disposable biobattery platforms has predominantly focused on specialized Gram-negative exoelectrogens such as *S. oneidensis*, *Geobacter sulfurreducens*, and *Pseudomonas aeruginosa*.<sup>[38,39]</sup> While these bacteria exhibit robust extracellular electron transfer (EET) capabilities and have demonstrated practical applications in microbial fuel cells, their potential cytotoxicity and environmental risks restrict their use to disposable devices requiring complete incineration. Consequently, they are unsuitable for transient, bioresorbable applications intended for medical or ecological settings, where safe biodegradation without adverse biological impact is essential. For instance, although *S. oneidensis* and *G. sulfurreducens* are non-pathogenic, their ability to reduce heavy metals raises environmental safety concerns.<sup>[38,39]</sup> *P. aeruginosa*, on the other hand, is an opportunistic pathogen<sup>[40]</sup> and is therefore not considered biocompatible or biosafe. Due to these biosafety limitations, Gram-negative exoelectrogens require strict containment and controlled disposal, making them unsuitable for transient, bioresorbable biobattery systems that must seamlessly degrade within the human body or nature.

In response to these limitations, Gram-positive bacteria, including spore-forming probiotics, have emerged as promising alternatives. Over the past decade, a growing number of Gram-positive bacteria have been identified with weak but functional EET capabilities.<sup>[21,23]</sup> Their superior biocompatibility, lack of endotoxins, and established safety in medical and food applications make them highly attractive biocatalysts for transient biomedical and environmental energy systems. *Bacillus subtilis*, a well-known probiotic and spore-forming bacterium, has recently demonstrated electrogenic behavior and has been used in biocatalytic applications within the human body, further supporting its potential for transient bioelectronic devices.<sup>[41,42]</sup> Its ability to remain dormant in spore form, survive extreme conditions, and

reactivate under favorable environments makes it an ideal candidate for transient biobattery applications.

Beyond *B. subtilis*, a broader range of commercial probiotic blends presents an exciting new avenue for biocatalysis in transient biobatteries. Many commercial probiotics, including strains from *Lactobacillus*, *Bifidobacterium*, and *Streptococcus*, are already formulated with protective encapsulation to enhance their stability and viability during storage and gastrointestinal transit. These encapsulated probiotics may serve as pre-packaged, controlled-release biocatalysts,<sup>[43,44]</sup> ensuring prolonged viability and electrochemical activity within transient biobattery systems. Importantly, probiotic blends, rather than individual probiotic strains, offer a more robust and adaptable bioelectrogenic platform. Bacteria naturally thrive and function in communities rather than as isolated individuals, and their collective behavior significantly influences survival, adaptation, ecological impact, and ultimately, electricity generation.<sup>[45,46]</sup> Harnessing this natural synergy enhances the electrogenic performance of transient biobatteries while leveraging the inherent stability and functionality of probiotic formulations. Moreover, using commercially available probiotic blends as biocatalysts streamlines the fabrication process, reducing both complexity and cost. These formulations are readily accessible, well-documented in terms of safety, and optimized for prolonged viability, eliminating the need for specialized microbial culturing. By utilizing probiotic blends as off-the-shelf biocatalysts, we can advance the development of scalable, low-cost, and sustainable transient biobattery platforms that align with medical and environmental applications.

In this study, we employed a comprehensive suite of analytical and experimental techniques to investigate the electrogenic properties of commercially available probiotic blends. Because Gram-positive bacteria typically possess a thick peptidoglycan cell wall that can impede EET,<sup>[23]</sup> the Gram-positive probiotic blends exhibited relatively weak but distinct redox peaks in cyclic voltammetry (CV) measurements on carbon electrodes (Figure 3a). Specifically, reduction peaks at approximately  $-0.6$  V and oxidation peaks at approximately  $+0.1$  V were observed, confirming their electrogenic capability. Notably, the reduction peak was more pronounced than the oxidation peak, indicating that the electrochemical reaction is largely irreversible. This suggests that the probiotic blends either favor the reduced state or rapidly consume the reduced species before they can be re-oxidized during the reverse sweep. Further supporting the slow and irreversible nature of electron transfer is the observation that the difference between the redox peaks increases with faster scan rates. In addition, the shift in peak potential with increasing scan rate once again points to a non-reversible mechanism, consistent with the inherent complexity of bacterial redox reactions at the electrode interface. Together, these findings underscore the potential of Gram-positive probiotic communities to serve as electrogenic agents, albeit with limited but measurable current-generating capacity under the conditions tested.

A modified electrode can substantially enhance bacterial EET by offering more favorable conditions for cells and their redox-active components to interact with the electrode surface. Previously, 3D hygroscopic hydrogel-based electrodes accelerated bacterial absorption and improved electrochemical performance with Gram-positive cells,<sup>[24]</sup> while embedded nanoparticles further enhanced conductivity and bacterial electron-transfer

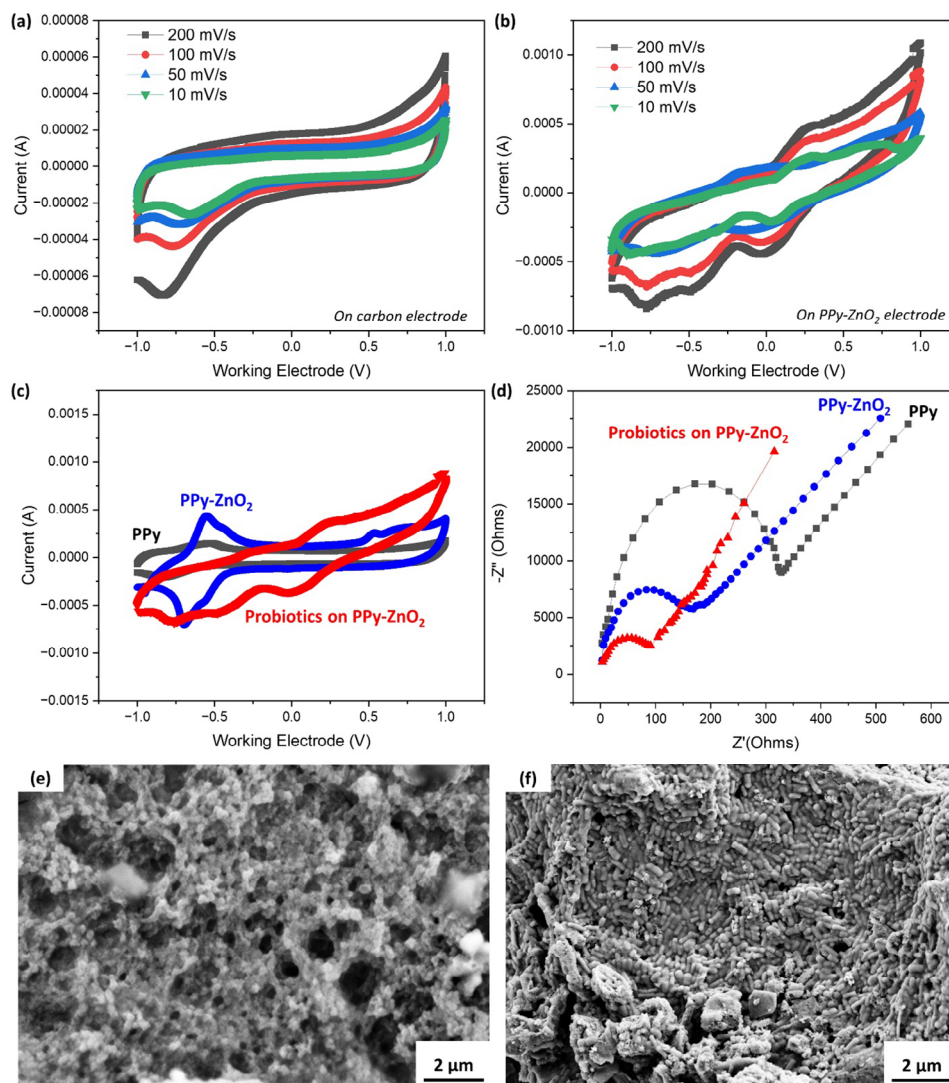


**Figure 3.** Assessing probiotic electrogenicity on different anodic materials. a) Cyclic voltammetry (CV) response curves of probiotic blends on a carbon electrode at varying scan rates. b) CV response curves of probiotic blends on a PPy-ZnO<sub>2</sub> composite electrode under different scan rates. c) Comparative CV profiles of various electrode materials, including PPy, PPy-ZnO<sub>2</sub>, and probiotic blends on a PPy-ZnO<sub>2</sub> electrode. d) Electrochemical impedance spectroscopy (EIS) analysis of the same electrode materials. e) Scanning electron microscopy (SEM) image of the PPy-ZnO<sub>2</sub> electrode surface without probiotics. f) SEM image of the PPy-ZnO<sub>2</sub> electrode after incorporating probiotic blends.

capacity.<sup>[25]</sup> However, in our proof-of-concept transient biobattery on dissolvable paper, the simple graphite electrode delivered exceedingly low power output—even with a well-characterized strong exoelectrogen (Figure 2). To overcome this limitation and improve electricity generation from probiotic blends with lower exoelectrogenic potential, we employed a conductive polymer, polypyrrole (PPy), conjugated with ZnO<sub>2</sub> nanoparticles (NPs) as the anodic electrode. PPy is capable of controlled degradation under specific conditions, and ZnO<sub>2</sub> NPs contribute biocompatibility, together forming a biodegradable electrode system. This combination not only enhances electrochemical performance but also supports transient functionality, which is crucial for sustainable, single-use biobatteries.

CV measurements of the PPy-ZnO<sub>2</sub> electrode showed more reversible behavior and significantly amplified redox peaks com-

pared to a carbon electrode (Figure 3b). These peaks remained relatively stable across various scan rates, with both reduction and oxidation peaks clearly observed. Furthermore, the PPy-ZnO<sub>2</sub> composite demonstrated superior electrochemical performance due to its intrinsic redox response compared to PPy alone (Figure 3c). When probiotic blends were introduced onto the PPy-ZnO<sub>2</sub> electrode, new redox peaks emerged distinct from those of the electrode itself, indicating robust electrogenic activity of the probiotics on this novel anode material (Figure 3c). Electrochemical impedance spectroscopy (EIS) further revealed a lower charge-transfer resistance ( $R_{ct}$ ), suggesting enhanced electron transfer at the electrode interface and confirming the robust electrogenic capability of these probiotic cells on the PPy-ZnO<sub>2</sub> composite electrode (Figure 3d; Figure S3, Supporting Information). In support of these findings, scanning electron microscopy



(SEM) images showed a dense layer of probiotic cells in direct contact with the porous composite surface (Figure 3e,f), providing a clear mechanistic basis for enhanced performance.

The probiotic blend examined in this study comprises 15 strains primarily from the genera *Lactobacillus* and *Bifidobacterium*, as well as *Streptococcus thermophilus*, *Pediococcus pentosaceus*, *Propionibacterium freudenreichii*, and *Saccharomyces boulardii*. Among these, *Lactobacillus* species are known to exhibit weak electron transfer capabilities,<sup>[47]</sup> whereas the electrogenic properties of the other strains have not yet been fully investigated. Consequently, we hypothesize that *Lactobacillus* strains are primarily responsible for electricity generation, while the remaining strains likely enhance this process by producing redox-active cofactors such as NADH and flavins. However, further studies are warranted to elucidate the EET pathways within these mixed communities and to explore the potential synergistic interactions among different species that may optimize collective electrogenic behavior.

### 2.3. Probiotic-Powered Biobatteries with pH-Responsive Biodegradation

The initial proof-of-concept dissolvable-paper biobattery demonstrated the viability of transient power devices but also highlighted several practical limitations. In particular, material choices and fabrication processes were severely restricted by the need to prevent premature disintegration of the water-soluble substrate, especially when handling liquid-phase PPy-ZnO<sub>2</sub> anodes or directly depositing aquatic probiotic samples. While this early design successfully produced a brief power output, its operating lifetime was limited to less than 30 min, and the device offered minimal control over activation under wet conditions. To overcome these constraints, dissolvable paper was encapsulated with EUDRAGIT EPO, a polymer sensitive to low pH (Figures 1c and 4a). This encapsulation protects against unintended dissolution during fabrication, enabling the integration of high-performance, water-based materials. An additional advantage of the low pH-sensitive encapsulation is the ability to trigger the device's activation or dissolution more precisely. The dissolvable paper was first coated with the pH-sensitive polymer, after which individual device components were fabricated on top (Figure 4b(i)). An additional external coating can be applied to the entire device to extend the operational time (Figure 4b(ii); Figure S4, Supporting Information). The commercial probiotic strains used in this work are originally covered with a neutral pH-sensitive coating to protect them from gastric acid and ensure they reach the intestines alive.<sup>[43,44]</sup> A crucial additional step was required to release these probiotics from their protective layer. Specifically, the microbes were pre-incubated in a neutral Luria-Broth (LB) medium, which removed the original coating, ensuring their selective activity in subsequent low-pH environments. After this step, the probiotics were mixed with the anodic PPy-ZnO<sub>2</sub> material and applied to the device.

However, vertically stacking the electrodes, as in the original configuration, is no longer feasible because the thick pH-sensitive polymer encapsulating the paper cannot function as an ion-exchange membrane between oppositely placed electrodes (Figure 2a). To overcome this limitation, we adopted a horizon-

tal interdigitated layout (Figure 4a), where all components are positioned on one side of the substrate (Figure S5, Supporting Information). In this configuration, a high-performance PPy-ZnO<sub>2</sub> anode containing probiotic blends is paired with a Prussian Blue-MnO<sub>2</sub> cathode, separated by a Nafion membrane. The MnO<sub>2</sub> in the cathode enhances electrochemical reduction by acting as an oxygenic cathode (Figure 4c,d), and can be chemically or biologically reduced to manganese ions, improving biocompatibility. While Nafion is neither biodegradable nor fully biocompatible, incorporating a small amount between the electrodes enables the overall device to disintegrate after use, effectively balancing enhanced electrochemical performance with transient functionality. This interdigitated approach also significantly improves design flexibility by adjusting and scaling the number of electrode legs (Figure 4a). To validate the effectiveness of the horizontal configuration with newly integrated materials for power generation and controllable transiency, we tested the device with four legs in a low pH solution (Figure 4a(i)). The device without the low-pH polymer encapsulation ceased functioning in water within 15 min (Figure 2b). Incorporating the single layer of the pH-sensitive membrane extended the operating time to 75 min—an approximate fivefold improvement (Figure 4b(i)). An additional external coating applied to the entire device extended the operational time over to 100 min; however, the extra diffusion barriers introduced by the coating slightly diminished peak performance (Figure S6, Supporting Information).

Figure 5 illustrates the biobattery's transient behavior upon immersion in pH 3.5 solution versus neutral-pH tap water. In tap water, the encapsulated biobattery remains intact, and protected by the pH-sensitive layer. In contrast, under acidic conditions (pH 3.5), the device gradually breaks down into small fragments over 160 min. The protective layer dissolves first, exposing the bio battery, activating it, and initiating power generation. Subsequently, the paper substrate disintegrates and, with it, all remaining components. Additionally, energy-dispersive X-ray spectroscopy (EDS) analysis of the dissolved materials after 160 min confirmed the presence of key biobattery components—including zinc (Zn), manganese (Mn), carbon (C), and oxygen (O)—validating the complete dissolution of the device in the solution (Figure S7a,b, Supporting Information). Although we did not specifically measure the degradation rates of individual components, the primary materials used, including Prussian Blue, MnO<sub>2</sub>, and ZnO<sub>2</sub>, are well-documented for their high biocompatibility and biosafety. Their degradation products are generally non-toxic and compatible with biological environments.<sup>[14,48,49]</sup> By selecting different pH-sensitive polymers or adjusting polymer chemistry, the activation window and degradation rate can be fine-tuned for applications such as precise medical diagnostics, targeted drug delivery, or environmental monitoring under specific pH conditions.

### 3. Future Direction

While this study successfully demonstrates the feasibility of a dissolvable probiotic-powered biobattery, several avenues remain open for future research. One promising direction involves developing biobattery stacks connected in series and parallel to power practical applications. Our current design was limited to a single biobattery to validate the proof-of-concept of probiotic

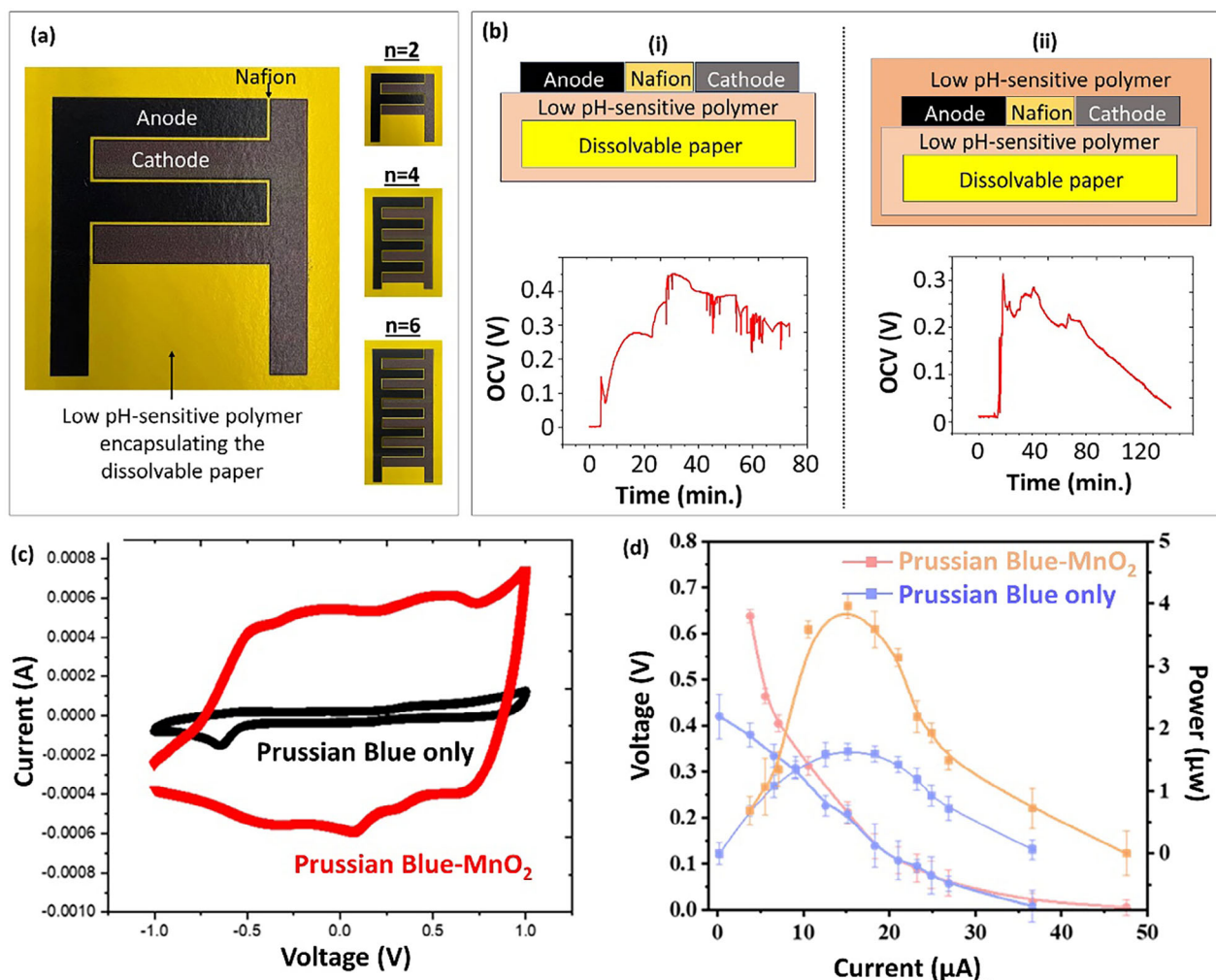


**Figure 4.** Probiotic-powered biobattery encapsulated with a low pH-sensitive polymer. a) Image of the horizontally configured probiotic-powered biobattery, demonstrating its scalability with varying numbers of electrodes. b) i. Cross-sectional schematic of the probiotic-powered biobattery ( $n = 4$ ) developed on a pH-sensitive polymer-encapsulated dissolvable paper substrate, along with its open-circuit voltage (OCV) over time when operating in a low-pH solution. (b) ii. Cross-sectional schematic of the probiotic-powered biobattery ( $n = 4$ ) encapsulated with an additional low pH-sensitive polymer, showing its OCV profile over time during operation. c) CV profile of the Prussian Blue cathode, comparing performance with and without  $\text{MnO}_2$  nanoparticles. d) Current-voltage ( $I$ - $V$ ) characteristics and power curve of the biobattery, comparing the Prussian Blue- $\text{MnO}_2$  composite cathode with a cathode containing Prussian Blue only.

electricity generation and to optimize performance and transiency. Expanding to multi-unit systems will require intensive research to manage and control transient behavior effectively. Moreover, future work should focus on creating fully integrated transient systems that incorporate an advanced, optimized biobattery stack. Such systems would demonstrate self-sustainability and complete dissolution after mission completion. It is also crucial to explore more biocompatible and biosafe materials to achieve a fully bioresorbable device. For instance, while the ion exchange membrane used in this study was employed in a minimal thin format to mitigate risk, it was not entirely biocompatible or biodegradable. Finally, future investigations should consider alternative pH-sensitive or enzymatically degradable encapsulation materials to tailor the operational lifetime of the biobattery for specific applications. In the biomedical domain, testing in simulated phys-

iological environments and animal models will be essential to assess both performance and safety for potential clinical applications.

## 4. Conclusion

The advancement of transient electronic systems necessitates the development of a compatible power source that operates for a predefined period and then safely disintegrates without leaving harmful residues. In this study, we presented a dissolvable probiotic-powered biobattery as a sustainable and biocompatible solution for transient applications. By utilizing commercially available probiotics as electrogenic biocatalysts, our biobattery ensured biosafety while providing a reliable energy source. Fabricated on a water-soluble paper substrate and encapsulated with a pH-sensitive coating, the device enabled precise control



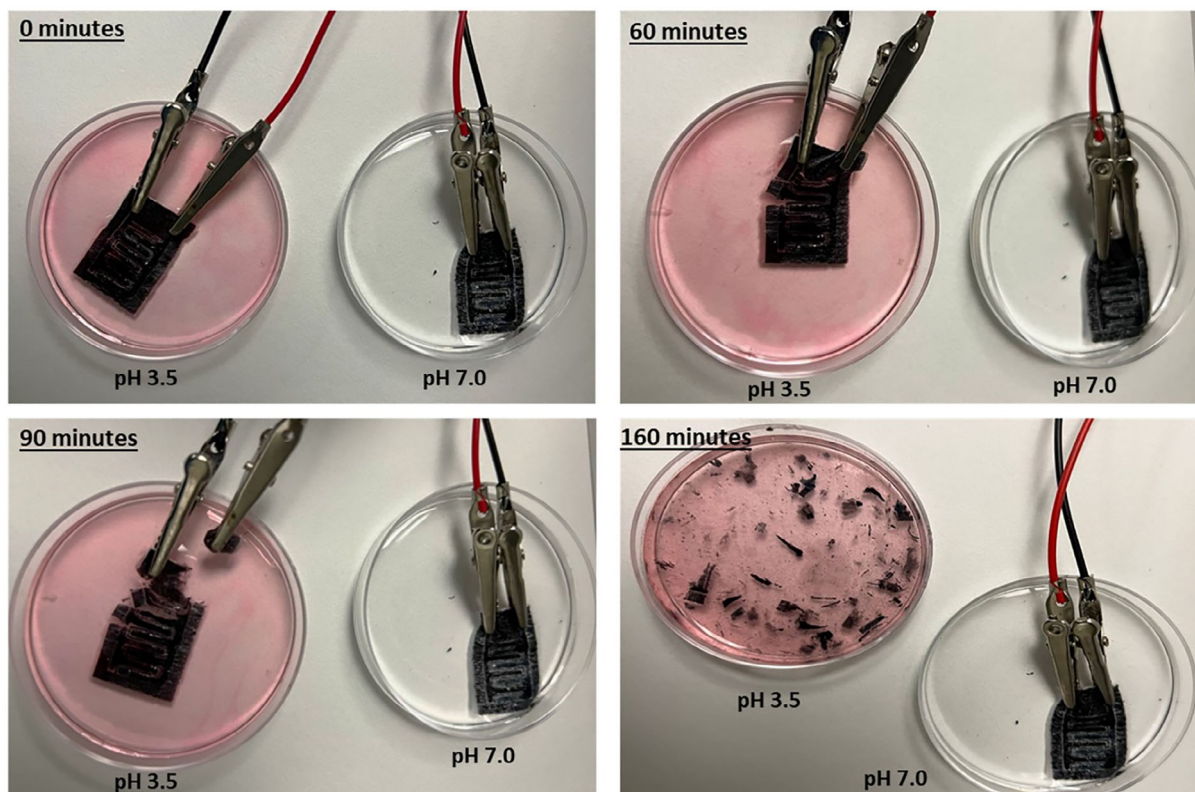


**Figure 5.** Transience evaluation of the biobattery ( $n = 6$ ) in pH 3.5 Solution and neutral-pH tap water. The dissolution behavior of the probiotic-powered biobattery was assessed in a low-pH (3.5) solution and neutral-pH tap water. After 160 min, the device completely dissolved in the pH 3.5 solution, demonstrating its pH-responsive transiency. In contrast, the biobattery remained structurally intact in neutral-pH tap water, highlighting its stability under physiological conditions.

over activation and dissolution. The integration of conductive polymer-polypyrrole with  $\text{ZnO}_2$  nanoparticles as an anodic material enhanced electron transfer efficiency, while Prussian Blue- $\text{MnO}_2$  composites in the cathode significantly improved electrochemical activity and thus overall power output of the biobattery. Furthermore, incorporating probiotic blends with electrogenic properties optimized energy output while maintaining environmental and biomedical safety. Our results demonstrate that this probiotic-powered biobattery can sustain power generation for an extended period while ensuring controlled biodegradation. This innovation represents a critical step toward fully transient, biore-sorbable energy systems, opening new possibilities for temporary medical implants, disposable sensors, and eco-friendly environmental monitoring solutions.

## 5. Experimental Section

**Probiotics:** The probiotic blend used in this study was purchased from Amazon and manufactured by NatureLife Labs. This formulation contains 15 specific strains, including *Lactobacillus acidophilus*, *Lactobacillus plantarum*, *Lactobacillus rhamnosus*, *Lactobacillus paracasei*, *Lactobacillus salivarius*, *Lactobacillus casei*, *Lactobacillus gasseri*, *Lactobacillus bulgaricus*, *Bifidobacterium animalis*, *Bifidobacterium breve*, *Bifidobacterium longum*, *Streptococcus thermophilus*, *Pediococcus pentosaceus*, *Propionibacterium freudenreichii*, and *Saccharomyces boulardii*. The probiotics are commercially encapsulated using delayed-release, pH-sensitive capsule technology, which

protects them from stomach acid and ensures their survival until they reach the intestines. To function optimally in a low-pH environment within a dissolvable paper encapsulated by a low-pH-sensitive membrane, the probiotics were first released from their original neutral-pH-sensitive membrane by pre-culturing them in a neutral pH LB medium. The LB medium was prepared by dissolving 10 g  $\text{L}^{-1}$  tryptone, 5 g  $\text{L}^{-1}$  sodium chloride, and 5 g  $\text{L}^{-1}$  yeast extract in 1 liter of deionized (DI) water. One milligram of probiotic powder was incubated in 5 mL of LB medium at 35 °C for  $\approx 1$  h.

**Shewanella Oneidensis:** *Shewanella oneidensis* MR-1 was used as a temporary biocatalyst for the proof-of-concept dissolvable biobattery. The bacteria were cultured in LB medium at 35 °C for 24 h until reaching an optical density at 600 nm ( $\text{OD}_{600}$ ) of 1.0, corresponding to  $\approx 10^9$  CFU  $\text{mL}^{-1}$ . After incubation, the cultures were centrifuged at 5000 rpm for 5 min and resuspended in a fresh LB medium. For freeze-drying, the LB medium was supplemented with 30% (v/v) glycerol (G33-1, Fisher Scientific, USA) to protect the cells. The suspension was then frozen overnight at  $-80$  °C (5708, Thermo Fisher Scientific, USA). Lyophilization was performed using the FreeZone Plus 2.5 Liter Cascade Benchtop Freeze Dry System (Lab-conco, USA) for 24 h at 0.04 mbar, following freezing and sublimation processes.

**Biofilm Fixation and SEM Imaging:** Bacterial cells were immobilized onto the anode using 2.5% glutaraldehyde in 0.1 M phosphate-buffered saline (PBS) and incubated overnight for fixation. After fixation, the samples were dehydrated through a graded ethanol series, and sequentially exposed to 35%, 50%, 75%, 95%, and 100% ethanol. Once dehydrated, they were left in a desiccator to dry overnight. The dried samples were then coated with a thin carbon layer using a 208HR Turbo Sputter Coater (Cressington Scientific Instruments, UK). Imaging and analysis were performed

using a field emission scanning electron microscope (FE-SEM, Supra 55 VP, Carl Zeiss AG, Germany).

**Fabrication of Dissolvable Biobattery on Water-Soluble Paper Substrate:** A proof-of-concept dissolvable biobattery was fabricated on a water-soluble paper substrate (SmartSolve Store, OH, USA) using a wax printing technique. Hydrophobic wax patterns were designed in AutoCAD and printed onto the dissolvable paper using a Xerox Phaser (ColorQube 8570) printer. The printed paper was then heated at 100 °C for 50 s, allowing the wax to melt into the substrate. This process defined the device boundaries, fluidic reservoir channels, and ion-exchange membrane while also reinforcing the paper to delay rapid dissolution in water (Figure 2b). For the anode, HB-grade pencil graphite (American Tombow Inc.) was manually drawn onto the pre-defined anodic microfluidic channels, forming a conductive graphite layer over the reservoir. This resulted in an average surface resistance of 310  $\Omega$  across the anodic channel. The cathode was constructed on the opposite side of the paper. After printing the wax-based ion-exchange membrane, a conductive pencil trace was drawn over it, followed by the deposition of the Prussian Blue-based cathode material. Prussian Blue was selected for its superior electrochemical stability and excellent catalytic efficiency in oxygen reduction reactions under neutral pH conditions.<sup>[50]</sup> Additionally, Prussian Blue is easily synthesizable, commercially available, and well-suited for transient and biodegradable applications.<sup>[51]</sup> Furthermore, the extensive prior research on biobatteries has validated its efficacy as a cathode material, with all relevant formulations readily accessible.<sup>[21,52]</sup> Each 1 cm<sup>2</sup> cathode contained 8 mg of Prussian Blue and 3 mg of graphene, dispersed in a conductive binder solution prepared by mixing: (i) 30  $\mu$ L of poly (3,4-ethylenedioxythiophene) polystyrene sulfonate (PEDOT:PSS) solution, (ii) 5  $\mu$ L of 5 wt.% Nafion, and (iii) 100  $\mu$ L of isopropanol. This mixture was ultrasonicated for 10 min before being brush-coated onto the pre-defined cathodic area of the paper (Figure 2b).

**Encapsulation of a Water-Soluble Paper Substrate with a pH-Sensitive Polymer:** A uniform low pH-sensitive polymer coating was applied to the water-soluble paper substrate using EUDRAGIT EPO. The encapsulation process involved the preparation of a homogeneous polymer solution and a controlled coating procedure to ensure uniform coverage. First, 1 gram of EUDRAGIT EPO was dissolved in 20 mL of ethanol under continuous stirring until a clear solution was obtained. To enhance solubility and maintain stability, 10 mL of DI water was gradually added while stirring. The pH of the solution was then carefully adjusted to pH 3.5 by adding acetic acid dropwise, with real-time monitoring using a pH meter. The solution was stirred for an additional 10–15 min to ensure homogeneity. For the coating process, the water-soluble paper was fully immersed in the prepared polymer solution and left to soak for 15 min. To achieve uniform coverage on both sides, the paper was carefully flipped using tweezers and soaked for another 15 min. After coating, the paper was gently removed, allowing excess liquid to drain off naturally. It was then suspended vertically using clips in a dust-free environment to facilitate even drying. The drying process was carried out at room temperature overnight, ensuring the formation of a stable and uniform encapsulation layer that effectively controls the dissolution behavior of the substrate.

**Fabrication of a Dissolvable Biobattery on a pH-Sensitive Polymer-Encapsulated Paper Substrate:** A horizontal interdigitated configuration was employed, where the anode and cathode were patterned in parallel on one side of the pH-sensitive polymer-encapsulated paper substrate. The electrochemical performance of both electrodes was enhanced by incorporating electrocatalytic composites—PPy-ZnO<sub>2</sub> for the anode and Prussian Blue-MnO<sub>2</sub> for the cathode. To prepare the PPy-ZnO<sub>2</sub> composite, 0.5 g of zinc acetate dihydrate was dissolved in 50 mL of DI water and stirred for 30 min to achieve a homogeneous solution. Next, 0.3 g of commercial PPy powder was added, followed by 15 min of sonication for uniform dispersion. The resulting suspension was transferred into a Teflon-lined stainless-steel autoclave and heated at 160 °C for 6 h. After cooling, the composite was filtered, washed thoroughly with DI water and ethanol, and dried at 60 °C for 12 h, yielding the PPy-ZnO<sub>2</sub> nanoparticle composite. For electrode deposition, a mixture of: (i) 1 mL of probiotic blend pre-incubated in LB medium, (ii) 5 mg of PPy-ZnO<sub>2</sub> composite, and (iii) 1 mL of PEDOT:PSS solution was screen-printed onto the predefined anode re-

gion of the substrate. The Prussian Blue-MnO<sub>2</sub> cathodic composite was synthesized using a hydrothermal method. First, 0.3 g of commercial Prussian Blue and 0.5 g of manganese sulfate monohydrate were dissolved in 50 mL of DI water with continuous stirring for 30 min. To adjust the pH and promote composite formation, 0.2 g of hydrochloric acid was added. The mixture was then transferred into a Teflon-lined autoclave and subjected to hydrothermal treatment at 150 °C for 8 h. After cooling, the resulting precipitate was filtered, washed thoroughly with DI water, and dried at 60 °C overnight, forming the Prussian Blue-MnO<sub>2</sub> nanoparticle composite. A 1:1 (w/w) ratio of the cathodic composite to PEDOT:PSS solution was screen-printed onto the predefined cathode region adjacent to the anode. The electrodes were then allowed to dry, ensuring a stable and uniform coating. To enhance ionic conductivity and electrode stability, 10  $\mu$ L of Nafion solution was applied to the region between the anode and cathode, followed by air drying. Finally, an additional external coating of the pH-sensitive polymer was applied to encapsulate the entire device, extending its operational lifespan.

**Electrical Characterization:** The electrical performance of the biobattery was rigorously assessed using a Data Acquisition System (Model DI-4108U, DataQ, USA). This system monitored the electrical output across various external resistors, ranging from high resistance to 0.35 k $\Omega$ , enabling precise voltage measurements essential for determining the OCV, *I*-*V* characteristics, and power output. Since the OCV represents the thermodynamic balance between the anode and cathode, it serves as a key indicator of biobattery performance. It effectively reflects the thermodynamic differences among bacterial strains in oxidizing organic substrates, offering insights into their electrochemical activity. The *I*-*V* and power curves were further analyzed to evaluate the biobattery's performance and assess the electrogenic capability of the bacterial samples.

**Electrochemical Characterization:** The electrochemical properties of the anodic and cathodic materials were systematically evaluated using CV and EIS. All measurements were conducted using a Squidstat Plus potentiostat (Admiral Instruments). A 0.5 M KCl buffer solution served as the electrolyte, while screen-printed carbon electrodes (Metrohm, USA) were used for the experiments. For CV measurements, the scan rate was set to 100 mV s<sup>-1</sup>, ensuring a balance between achieving sufficient resolution of the electrochemical processes and minimizing capacitive current effects. The potential window was carefully selected to encompass the redox-active regions of the materials and bacterial strains, enabling a detailed characterization of their electrochemical behavior. CV analysis provided valuable insights into the redox characteristics and charge transfer properties of the materials. EIS testing was performed to assess the impedance properties across a broad frequency range (0.1–10 kHz), providing a deeper understanding of the materials' resistance and capacitive behavior. The resulting Nyquist plot (Figure S3, Supporting Information) can be analyzed by using an equivalent circuit model, which included: (i) solution resistance (*R*<sub>s</sub>) – representing the resistance of the electrolyte, (ii) charge transfer resistance (*R*<sub>ct</sub>) – indicating the difficulty of electron transfer at the electrode interface, and (iii) double-layer capacitance (*C*<sub>dl</sub>) – reflecting the electrochemical interface's capacitive behavior. The Nyquist plot exhibited a small semicircle in the high-frequency region, followed by a linear segment at lower frequencies, indicative of capacitive behavior with rapid electron transfer. In this study, particular emphasis was placed on charge transfer resistance (*R*<sub>ct</sub>) to assess bacterial EET to the selected anodic materials. To ensure accuracy and reproducibility, each measurement was repeated multiple times.

**Statistical Analysis:** All experimental data presented in this study were obtained from a minimum of three independent replicates to ensure reliability and reproducibility. Results are expressed as mean  $\pm$  standard error (SE) unless otherwise stated. All statistical analyses were conducted using Origin (OriginLab, USA) to ensure precision in data interpretation and graphical representation.

## Supporting Information

Supporting Information is available from the Wiley Online Library or from the author.

## Acknowledgements

This research was funded by the National Science Foundation (Grant Nos. 2410431 and 2246975) and supported by the SUNY System Administration through the SUNY Research Seed Grant Award (Grant No. 241000). The authors sincerely appreciate the Analytical and Diagnostic Laboratory at SUNY Binghamton for granting access to their facilities. Additionally, ChatGPT was used during manuscript preparation to assist in identifying and correcting grammatical errors, with final revisions ensuring accuracy and clarity. The authors assume full responsibility for the content and conclusions presented in this publication.

## Conflict of Interest

The authors declare no conflict of interest.

## Data Availability Statement

The data that support the findings of this study are available from the corresponding author upon reasonable request.

## Keywords

biocompatible, bioresorbable electronics transient biobattery, biosafe, probiotic biocatalysts, transient electronics

Received: February 28, 2025

Revised: March 12, 2025

Published online: March 26, 2025

- [1] S. Hwang, S. Kang, X. Huang, M. A. Brenckle, F. G. Omenetto, J. A. Rogers, *Adv. Mater.* **2015**, 27, 47.
- [2] H. Bae, B. Lee, D. Lee, M. Seol, D. Kim, J. Han, C. Kim, S. Jeon, D. Ahn, S. Park, J. Park, Y. Choi, *Sci. Rep.* **2016**, 6, 38324.
- [3] A. Fanelli, D. Ghezzi, *Curr. Opin. Biotechnol.* **2021**, 72, 22.
- [4] J. Shim, J. A. Rogers, S. Kang, *Mater. Sci. Eng.: R: Rep.* **2021**, 145, 100624.
- [5] X. Yu, W. Shou, B. K. Mahajan, X. Huang, H. Pan, *Adv. Mater.* **2018**, 30, 1707624.
- [6] Y. Zhang, G. Lee, S. Li, Z. Hu, K. Zhao, J. A. Rogers, *Chem. Rev.* **2023**, 123, 11722.
- [7] M. Irimida-Vladu, E. D. Glowacki, G. Voss, S. Bauer, N. S. Saricic, *Mater. Today* **2012**, 15, 340.
- [8] R. Jamshidi, M. Taghavimehr, Y. Chen, N. Hashemi, R. Montazami, *Adv. Sustainable Syst.* **2022**, 6, 2100057.
- [9] M. P. Cenci, T. Scarazzato, D. D. Munchen, P. C. Dartora, H. M. Veit, A. M. Bernardes, P. R. Dias, *Adv. Mater. Technol.* **2022**, 7, 2001263.
- [10] L. Dong, L. Shan, Y. Wang, J. Liu, *Supramolecular Mater.* **2025**, 4, 100082.
- [11] K. Rajaram, S. M. Yang, S. Hwang, *Adv. Energy. Sustainability Res.* **2022**, 3, 2100223.
- [12] J. P. Esquivel, P. Alday, O. A. Ibrahim, B. Fernández, E. Kjeang, N. Sabaté, *Adv. Energy Mater.* **2017**, 7, 1700275.
- [13] Y. Chen, R. Jameshidi, K. White, S. Cinar, E. Gallegos, N. Hashemi, R. Montazami, *J. Polym. Sci., Part B: Polym. Phys.* **2016**, 54, 2021.
- [14] K. Fu, Z. Wang, C. Yan, Z. Liu, Y. Yao, J. Dai, E. Hitz, Y. Wang, W. Luo, Y. Chen, M. Kim, L. Hu, *Adv. Energy Mater.* **2016**, 6, 1502496.
- [15] H. Xi, D. Chen, L. Lv, P. Zhong, Z. Lin, J. Chang, H. Wang, B. Wang, X. Ma, C. Zhang, *RSC Adv.* **2017**, 7, 52930.
- [16] Q. Zheng, Y. Zou, Y. Zhang, Z. Liu, B. Shi, X. Wang, Y. Jin, H. Ouyang, Z. Li, Z. L. Wang, *Sci. Adv.* **2016**, 2, 1501478.
- [17] S. Choi, *Batteries* **2023**, 9, 119.
- [18] S. Choi, *Small* **2022**, 18, 2107902.
- [19] A. Naha, R. Debroy, D. Sharma, M. P. Shah, S. Nath, *Cleaner and Circular Bioeconomy* **2023**, 5, 100050.
- [20] B. E. Rittmann, *Biotechnol. Bioeng.* **2008**, 100, 203.
- [21] M. Mohammadifar, M. Tahernia, J. H. Yang, A. Koh, S. Choi, *Nano Energy* **2020**, 75, 104994.
- [22] Y. Gao, M. Rezaie, S. Choi, *Nano Energy* **2022**, 104, 107923.
- [23] M. Tahernia, E. Plotkin-Kaye, M. Mohammadifar, Y. Gao, M. Oefelein, L. Cook, S. Choi, *ACS Omega* **2020**, 5, 29439.
- [24] M. Rezaie, Z. Rafiee, S. Choi, *Adv. Energy Mater.* **2023**, 13, 2202581.
- [25] M. Rezaie, Z. Rafiee, S. Choi, *Adv. Sustainable Syst.* **2024**, 8, 2300357.
- [26] M. Rezaie, S. Choi, *Small* **2023**, 19, 2301125.
- [27] Y. Gao, M. Mohammadifar, S. Choi, *Adv. Mater. Technol.* **2019**, 4, 1970039.
- [28] M. Mohammadifar, I. Yazgan, J. Zhang, V. Kariuki, O. Sadik, S. Choi, *Adv. Sustainable Syst.* **2018**, 2, 1800041.
- [29] Y. Gao, S. Choi, *Adv. Mater. Technol.* **2018**, 3, 1800118.
- [30] M. Landers, S. Choi, *Nano Energy* **2022**, 97, 107227.
- [31] J. H. Cho, Y. Gao, J. Ryu, S. Choi, *ACS Omega* **2020**, 5, 13940.
- [32] S. Choi, *Biosens. Bioelectron.* **2015**, 69, 8.
- [33] Z. Rafiee, A. Elhadad, S. Choi, *Adv. Sustainable Syst.* **2024**, 8, 2400049.
- [34] M. Landers, A. Elhadad, M. Rezaie, S. Choi, *ACS Appl. Mater. Interfaces* **2022**, 14, 45658.
- [35] S. Ikeda, Y. Takamatsu, M. Tsuchiya, K. Suga, Y. Tanaka, A. Kouzuma, K. Watanabe, *Essays Biochem.* **2021**, 65, 355.
- [36] S. Wenfeng, R. Gooneratne, N. Glithero, R. J. Weld, N. Pasco, *Appl. Microbiol. Biotechnol.* **2013**, 97, 10189.
- [37] M. Mohammadifar, S. Choi, *Adv. Mater. Technol.* **2017**, 2, 1700127.
- [38] V. Sharma, P. P. Kundu, *Enzyme Microb. Technol.* **2010**, 47, 179.
- [39] P. Jalili, A. Ala, P. Nazari, B. Jalili, D. D. Ganji, *Heliyon* **2024**, 10, 25439.
- [40] Z. Rafiee, M. Rezaie, S. Choi, *Biosens. Bioelectron.* **2022**, 216, 114604.
- [41] J. Ryu, S. Choi, *Biosens. Bioelectron.* **2021**, 186, 113293.
- [42] J. Ryu, M. Landers, S. Choi, *Biosens. Bioelectron.* **2022**, 205, 114128.
- [43] F. J. Rodrigues, M. F. Cedran, J. L. Bicas, H. H. Sato, *Food Res. Int.* **2020**, 137, 109682.
- [44] Q. Sun, S. Yin, Y. He, Y. Cao, C. Jiang, *Nanomaterials* **2015**, 13, 2023.
- [45] M. E. Hibbing, C. Fuqua, M. R. Parsek, S. B. Peterson, *Nat. Rev. Microbiol.* **2010**, 8, 15.
- [46] L. L., M. Mohammadifar, A. Elhadad, M. Tahernia, Y. Zhang, W. Zhao, S. Choi, *Adv. Energy Mater.* **2021**, 11, 2100713.
- [47] J. V. Boas, V. B. Oliveira, L. R. C. Marcon, M. Simoes, A. M. F. R. Pinto, *Sci. Total Environ.* **2019**, 648, 263.
- [48] N. Chakraborty, I. Roy, P. Kumar, S. Singh, R. Pathak, V. Gautam, H. K. Gautam, *Pharmaceutics* **2024**, 16, 1616.
- [49] S. G. Balwe, D. Moon, M. Hong, J. M. Song, *Nano Convergence* **2024**, 11, 48.
- [50] M. Blasco-Ahicart, J. Soriano-López, J. J. Carbó, J. M. Poblet, J. R. Galán-Mascarós, *J. Am. Chem. Soc.* **2016**, 138, 10132.
- [51] J. Peng, W. Zhang, Q. Liu, J. Wang, S. Chou, H. Liu, S. Dou, *Adv. Mater.* **2022**, 34, 2108384.
- [52] M. Mohammadifar, S. Choi, *J. Power Sources* **2019**, 429, 105.